# Mechanical properties and water absorption behaviour of PLA and PLA/wood composites prepared by 3D printing and injection moulding

*Josef Valentin Ecker, Andreas Haider, Ivana Burzic and Axel Huber*
WPC, Wood K plus, Linz, Austria, and
*Gerhard Eder and Sabine Hild*
Institute of Polymer Science, Johannes Kepler Universität Linz, Linz, Upper Austria, Austria

**Abstract**

**Purpose** – This papers aims to study the influence of water absorption on the mechanical properties of poly lactic acid (PLA) and PLA/Wood composites. Virgin PLA and PLA/Wood double-bone-shaped specimens were prepared by two methods: injection moulding and 3D printing. The results were compared to each other and showed the influence of the production method on the properties of the produced parts.

**Design/methodology/approach** – Morphology studies were done by scanning electron microscopy (SEM) from fracture surfaces of tensile and notched impact specimens of all samples. Tensile properties were analysed by the production and testing of dog-bone-shaped samples. Heat deflection temperature (HDT) was tested, as also was the crystallinity of the tested samples by differential scanning calorimetry.

**Findings** – The values for notched impact strength were higher upon water uptake in the case of injection-moulded specimens, which was not the case with 3D-printed specimens. Tensile properties of the specimens produced by both methods were reduced after water absorption tests. Values of the HDT were also lower after water absorption tests studied for both processing methods.

**Originality/value** – Morphology studies were done by SEM from fracture surfaces of tensile as well as notched impact specimens of injection-moulded and 3D-printed samples. The effect of water storage on various samples was tested. The two different production technologies were compared to each other owing to their influence of water storage. This study also dealt with NFC compounds and produced NFC composites and the influence of water storage on these samples.

**Keywords** 3D-FLM-printing, Biopolymers

**Paper type** Research paper

## 1. Introduction

Recently there has been a growing interest in the development of environmental-friendly polymer composites based on biodegradable poly lactic acid (PLA) and various natural-based fillers such as cellulose, flax, kenaf as well as wood fibres. The addition of such natural-based fillers to PLA can improve its mechanical properties without affecting its biodegradability. Owing to the occurrence of polar oxygen linkages, PLA is naturally a hydrophilic polymer. However, through the existence of methyl side groups, PLA also exhibits a hydrophobic character (Vroman and Tighzert, 2009). Notably, this natural hydrophilicity is responsible for its moderate decomposition in accordance with the surrounding moisture and temperature. The first stage of PLA degradation by hydrolysis leads usually to a reduction of its molecular weight to values below 10 kDa before it becomes biodegradable (Ndazi and Karlsson, 2011). Previous studies have shown that PLA is moderately stable in water at mesophilic temperatures (15-40°C), at which it can absorb between 0.7 and 1 per cent of water in 30 days (Yew *et al.*, 2005) or slightly more at longer immersion periods (Taib *et al.*, 2009). However, the absorption of water by PLA biocomposites at such temperatures can lead to moderate changes in their properties, depending on filler content (Taib *et al.*, 2009). As hydrolysis of PLA is influenced by ambient moisture and temperature, it is possible to accelerate the diffusion of water and thereby increase its hydrolysis by subjecting it to thermophilic temperatures above 50°C. In general, the nature of the polymer and the ageing conditions play a role in the ageing behaviour of biocomposites. With regard to mechanical properties, both the matrix polymers and their biocomposites are affected by hydrothermal ageing. For example, in case of rice starch (20 per cent)/PLA biocomposites, which were aged in water at 30°C for 30 days, the tensile modulus dropped from 3.8 to 2.1 GPa. At the same time, its stress at break reduced from 44 to 30 MPa and its strain at failure, from 2.5 to 2.2 per cent (Yew *et al.*, 2005). The

The current issue and full text archive of this journal is available on Emerald Insight at: **www.emeraldinsight.com/1355-2546.htm**

Rapid Prototyping Journal
25/4 (2019) 672–678
 [ISSN 1355-2546]
[DOI 10.1108/RPJ-06-2018-0149]

This work was supported by the European Regional Development Fund and the province of Upper Austria through the programs IWB 2014-2020 – Upper Austria (project Biorest) and INTERREG V-A Österreich – Deutschland/Bayern 2014-2020 (project TFP Hy-Mat AB97).

Received 18 June 2018
Revised 2 September 2018
10 October 2018
Accepted 25 October 2018

changes in PLA properties contributed to these changes. Under the same conditions, the PLA modulus dropped from 3.3 to 2.9 GPa, failure stress dropped from 58 to 54 MPa and failure strain, from 3.8 to 3.2 per cent. Drying of samples recovered stiffness but not strength. Yew *et al.* concluded that both reversible (physical) and irreversible (chemical) changes are involved in wet ageing of PLA and its composites. When natural fibres are used to reinforce polymers, the decline in properties is often quite large (Alvarez *et al.*, 2004), as these fibres are generally sensitive to water. Several authors have indicated this sensitivity, which is much larger than that of glass fibres exposed to similar wet environments (Retegi *et al.*, 2006). According to their composition, the latter may undergo stress corrosion cracking, which requires a particular combination of load and environment.

In this study, an influence of water absorption on mechanics and morphology of PLA and PLA/wood composites prepared by two different methods, injection moulding and 3D printing, is reported. Morphology studies were performed by scanning electron microscopy (SEM), and the results were linked to the mechanical performance of PLA as well as PLA/wood composites, before and after water absorption. The results from this work could be further used to guide the selection of the manufacture methods between 3D printing and injection moulding of PLA itself and PLA biocomposites.

## 2. Experimental

### 2.1 Materials and methods

*2.1.1 Materials*

In the present study, the PLA type Ingeo 3251 D from NatureWorks LLC, a low-viscosity injection-moulding grade with MFR 210°C/2.16 kg = 80 g10min$^{-1}$, was used as the base material. For PLA reinforcement, wood flour with trade name Arbocel C100, supplied by Rettenmaier&Söhne GmbH&CoKG, was used. An overview of the tested PLA and PLA/wood composites is presented in Table I.

*2.1.2 Sample preparation*

*2.1.2.1 Compounding.* Prior to compounding, both wood flour and PLA were dried at 60°C for 12 h. After drying, the components were compounded by lab scale twin screw extruder from Brabender, with a screw diameter of D = 20 mm and a length of 40D. For pelletizing, the Econ Underwater Pelletizing System EUP50 was used. The pellets were dried at 60°C for 12 h before further processing.

**Table I** List of abbreviations and formulations of the tested PLA and PLA/wood composites

| Code | PLA content [Wt.%] | Wood content [Wt.%] | Sample preparation method |
|---|---|---|---|
| PLA_IM | 100 | 0 | Injection moulding |
| PLA_3D | 100 | 0 | 3D printing |
| PLA/15W_IM | 85 | 15 | Injection moulding |
| PLA/15W_3D | 85 | 15 | 3D printing |
| PLA/30W_IM | 70 | 30 | Injection moulding |
| PLA/30W_3D | 70 | 30 | 3D printing |

*2.1.2.2 Injection moulding and 3D-fused layer modelling (FLM)-printing process.* After the compounding step, double bone specimens were produced by two methods, injection moulding as well as 3D-FLM printing, respectively. For injection moulding, an injection-moulding machine, Battenfeld HM1300-350 was used, with a screw diameter of 35 mm and a length-to-diameter ratio (L/D) of 22. The polymer melt was injected at a temperature of 190°C with 50 cm$^3$/s and rotational screw speed of 250 mm/s. The mould temperature was set to 25°C.

At 3D-FLM-printing, the filament was processed using a 0.6 mm diameter die. The layer height was 0.3 mm and the print speed was 50 mm/s at a temperature of 205°C. Prior to the 3D-FLM printing process, filaments were produced from the granules by filament-extrusion process. This was conducted at a conical twin screw extruder from Brabender.

All the samples prepared by injection moulding as well as 3D printing were then annealed in an oven at 105°C for 1 h.

*2.1.2.3 Water-absorption tests.* The samples were stored in clean tap water at room temperature. The samples were fully covered by the water during the absorption test. After defined intervals, the samples were taken out of the water to measure their geometry (length, width and height) as well as their weights. In total, the samples were stored in water for seven days.

*2.1.2.4 Mechanical testing.* A mechanical-testing machine (BETA 20-10/4 × 11.) was used to measure the properties tensile modulus ($T_{mod}$), tensile strength ($T_{str}$) and tensile strain ($T_{\varepsilon}$) according to ASTM Standard D 638. System control and data analysis were performed with Datum software. The un-notched and notched Charpy impact strength were measured with a monitor/impact machine from Instron CEAST 9050 according to ASTM D 256. All presented results are mean values of ten independent measurements.

*2.1.2.5 Morphological analysis.* The morphology of the unfilled PLA and its composites was observed with SEM. A Phenom ProX desktop SEM microscope with a field-emission gun and accelerating voltage of 10 kV was used. The samples were viewed perpendicularly to the fractured surface.

*2.1.2.6 Thermal analysis.* The crystallinity of the PLA specimens was determined by differential scanning calorimetry (DSC) analysis, using a DSC 1 from Mettler Toledo, equipped with a gas controller GC 200. Samples of about 5 mg were placed in hermetic aluminium pans. First, a heating ramp from 30 to 200°C was applied with a rate of 10 K/min, followed by a cooling scan from 200 to 30°C with the same rate. Next, the ramp from 30 to 200°C was run a second time. Crystallinity ($X_c$) was then calculated using the following formula (Lorenza *et al.*, 2007):

$$X_C = \frac{\Delta H_m - \Delta H_{cc}}{\Delta H_m^0} \times 100 \quad (1)$$

where, $\Delta H_m$ is the melting enthalpy of PLA samples calculated from the first thermal scan, $\Delta H_{cc}$ is the enthalpy of cold crystallisation and $\Delta H^0{}_m$ represents the theoretical melting enthalpy of 100 per cent crystalline PLA, given as 93 Jg$^{-1}$ in Hoogsteen *et al.* (1990).

## 3. Results and discussion

The results of water absorption tests for PLA and PLA/wood composites prepared by injection moulding and 3D printing are shown in Figure 1.

The results were characterised as follows. The time for the water uptake equilibrium was about 140-160 h of water storage. The different samples showed similar equilibration times. Neither the difference in material combination nor the fabrication method influenced this equilibration time. Additional storage time did not lead to further mass increase for the injection-moulded samples. Therefore, the measurement was stopped after 160 h.

The 3D-printed samples showed faster water uptake behaviour than injection-moulded samples. The total amount of weight gain because of water uptake was also higher for 3D-printed samples. Therefore, different fabrication processes strongly influenced the water uptake behaviour. Those results could be explained by the porous structure of the PLA specimen produced in 3D printing, as depicted by computer tomography (CT) measurements in Figure 2 (Ecker *et al.*, 2017).

**Figure 1** Weight change of samples over water storage time at room temperature (RT)

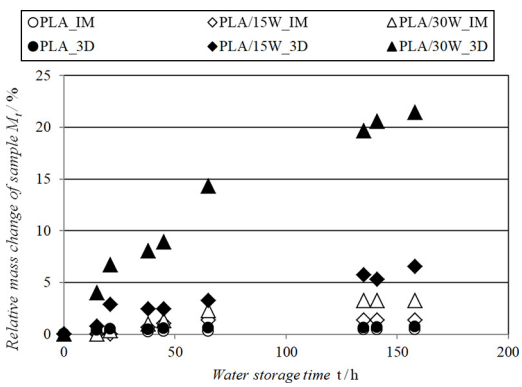


**Figure 2** CT scan of cross section of 3D printed sample (top) and injection moulded sample (bottom)

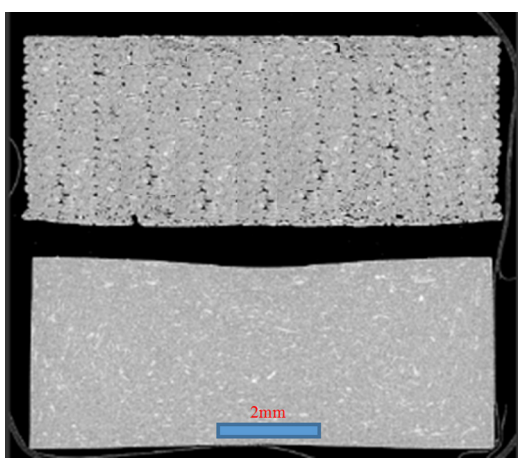


Besides the fabrication method, the total amount of wood content in the compound also influenced the water uptake behaviour of the tested samples. With increasing wood content, the water uptake increased over time, as also the total weight gain at water uptake equilibrium. Within the injection-moulded samples, the influence of wood content on the water uptake behaviour was not as distinctive compared to the 3D-printed samples. The total amount of weight gain increased from 6 Wt.% for PLA/15W to more than 20 Wt.% of mass change for PLA/30W in the case of 3D-printed specimens. The lowest total water uptake was recorded for the injection-moulded sample containing no wood.

In general, the addition of wood flour induced higher water absorption capability, regardless of the preparation method. This was already reported in the literature before for PLA composites (Huda *et al.*, 2006).

### 3.1 Mechanical properties of the PLA/wood composites

In the next step, the influence of water storage on the mechanical properties of PLA/wood composites was analysed. The results of mechanical properties tensile strength ($T_{str}$) and tensile modulus ($T_{mod}$) are shown in Figure 3.

The tensile properties for PLA and PLA/wood composites were strongly influenced by the fabrication method (Figure 3). Injection-moulded samples showed higher tensile strength, tensile strain and tensile modulus values than 3D-printed samples in the case of both unfilled PLA as well as its composites. After storing the samples in water, the tensile strength as also the tensile strain decreased for all composites, whereas the unfilled PLA specimens showed no significant loss in tensile strength or tensile strain. Tensile properties were not significantly altered by water storage. Therefore, the decrease of the tensile properties of PLA/wood composites after water uptake could be addressed to the wood flour used for PLA reinforcement in this study. This observation was already reported in the literature for other PLA composites (Huda *et al.*, 2006).

Increasing the wood content led to a higher tensile modulus in injection-moulded samples. In contrast, the 3D-printed samples showed a minor reduction of the tensile modulus at higher wood content. The reason for that could be the porous structure of 3D-printed specimens as obtained from CT analysis (Figure 2).

Unfilled PLA specimens prepared by injection moulding again showed higher impact strength and notched impact strength values than 3D-printed samples (Figure 4). Those differences could be again attributed to the different structure of the specimens produced by both methods. After storage of PLA specimens in water, impact strength values were equal or slightly higher for both injection-moulded and 3D-printed samples.

As shown in SEM images of tested samples (Figure 5), there were obvious differences in the structure of PLA samples produced by 3D printing and injection moulding. The SEM images of unfilled PLA specimens before and after storage in water did not show any significant differences. With regard to injection-moulded samples, the increase of wood content reduced the impact strength. The 3D-printed samples showed a similar behaviour – the impact strength was reduced by 30 per cent at the higher wood content. The values of notched impact

**Figure 3** Tensile strength (a), tensile strain (b) and tensile modulus (c) of PLA and PLA/Wood composites prepared by injection moulding and 3D printing

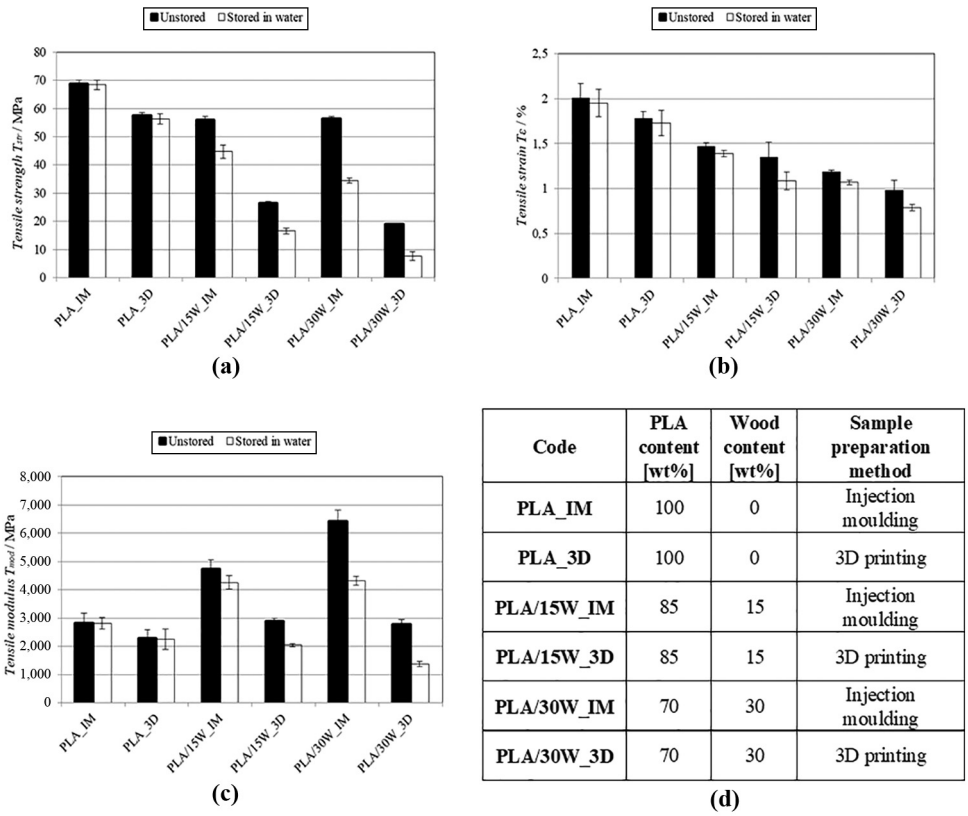


| Code | PLA content [wt%] | Wood content [wt%] | Sample preparation method |
|---|---|---|---|
| PLA_IM | 100 | 0 | Injection moulding |
| PLA_3D | 100 | 0 | 3D printing |
| PLA/15W_IM | 85 | 15 | Injection moulding |
| PLA/15W_3D | 85 | 15 | 3D printing |
| PLA/30W_IM | 70 | 30 | Injection moulding |
| PLA/30W_3D | 70 | 30 | 3D printing |

**Notes:** (a) Tensile strength $T_{str}$; (b) Tensile strain $T_{\varepsilon}$; (c) Tensile modulus $T_{mod}$; (d) Legend declaration

**Figure 4** Impact strength IS (a) and notched impact strength NIS (b) of PLA and PLA/Wood composites prepared by injection moulding and 3D printing

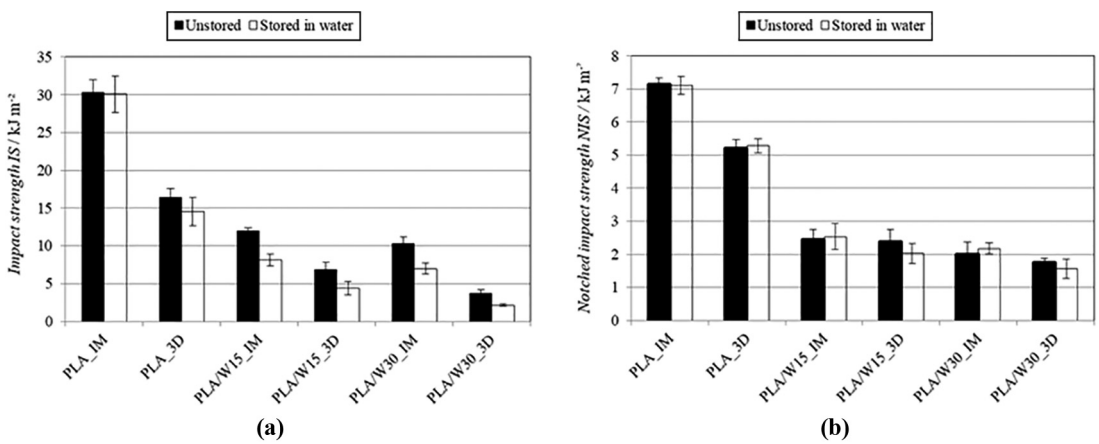


**Notes:** (a) Impact strength IS; (b) notched impact strength NIS

strength for PLA/wood composite were less influenced by the fabrication method. Injection-moulded samples had slightly higher notched impact strength values than 3D-printed samples. For all samples, the increase of wood content reduced the impact strength. All PLA/wood composites showed different behaviour upon water uptake experiments. The values of notched impact strength of injection-moulded samples increased upon water storage. This effect increased with increasing wood content. The notched impact strength values for 3D-printed samples were reduced upon water storage. This

**Figure 5** SEM images of fracture surface of notched impact specimens of virgin PLA unstored (a, c) and stored (b, d) in water prepared by 3D printing (a, b) and injection molding (c, d)

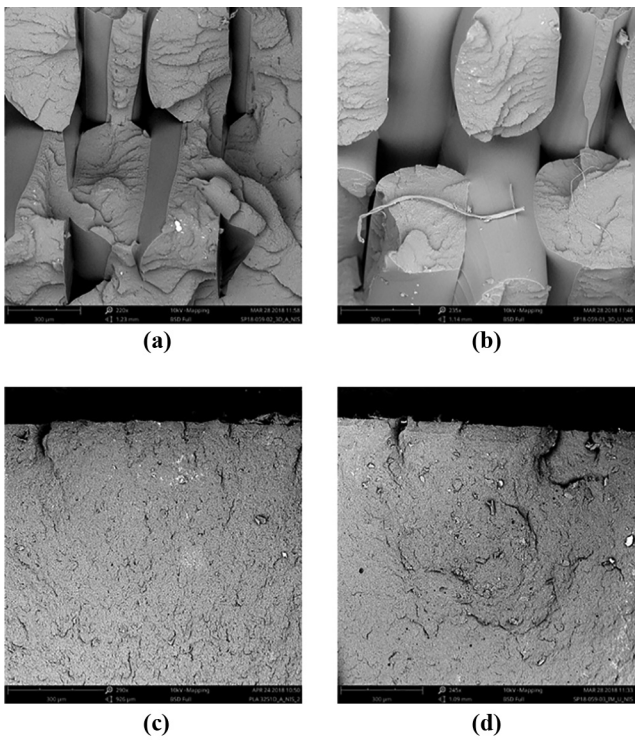


**Notes:** (a) PLA_3D_U (unstored); (b) PLA_3D_S (stored); (c) PLA_IM_U (unstored); (d) PLA_IM_S (stored)

**Figure 6** SEM images of fracture surfaces of notched impact specimens of PLA/Wood composites unstored (a, c) and stored (b, d) in water prepared by 3D printing (a, b) and injection moulding (c, d)

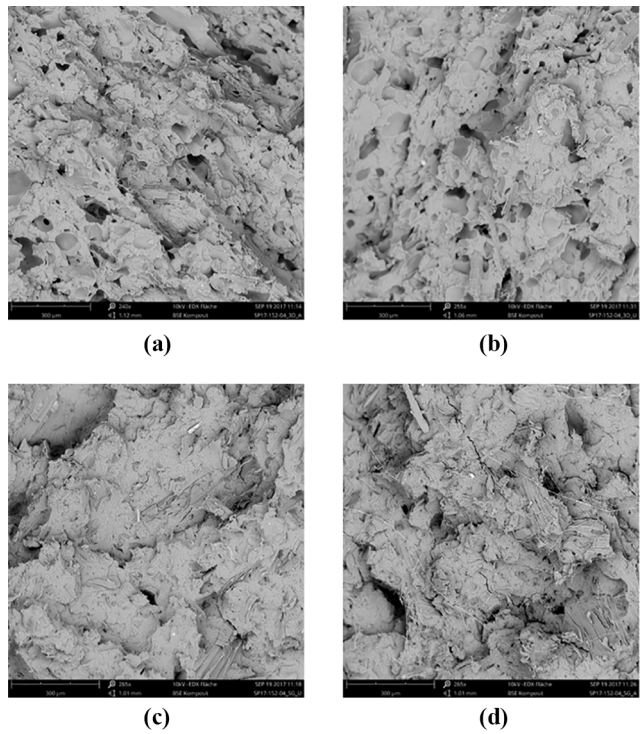


**Notes:** PLA/15W_3D_U (unstored); (b) PLA/15W_3D_S (stored); (c) PLA/15W_IM_U (unstored); (d) PLA/15W_IM_S (stored)

conspicuous behaviour of injection-moulded samples was studied in detail. Figure 6 shows SEM images of fracture surfaces for notched impact specimen of PLA/15W injection-moulded and 3D-printed specimens un-stored [Figure 6(a)] and stored [Figure 6(b)] in water with 300 $\mu$m scale bar. In general, the samples showed good homogeneity. No wood particle agglomeration could be located.

SEM images of both PLA/15W_IM and PLA/30W_IM showed special differences in structure after water storage. Fibril structure on the nanometre scale, recorded at the fracture surfaces of PLA/wood composites that come from deformed crystals upon fracture, could only be found in the samples stored in water processed by injection moulding. Those fibrils could not be found in the case of 3D-printing samples. Main differences could be attributed to the different cooling and deformation conditions in these two processes. In the literature, it is well known that tie molecules concentration is largely dependent on the degree of super-cooling and molecular weight. The number of tie molecules was larger in the quenched materials because the number of nuclei for crystallisation increases and crystal thickness decreases with the degree of super-cooling (Seguela, 2005). When an impact load is applied to a network of crystal and tie molecules, the tie molecules pull on the crystals and the crystals are unravelled along the impact direction, which enable crystallites to be transformed into fibrils on the scale of a few hundreds of nanometres, forming crazes. Finally, fracture occurs in the fibrils of a craze (Yang *et al.*, 2012). This could have exactly been the case in the PLA/wood composites produced by injection moulding. In general, during injection moulding, owing to very fast cooling, PLA material could not crystallise. The used mould temperature was set to 25°C. Therefore, in the tested samples, final crystallinity values of 42.1 per cent in the case of unfilled PLA were reached by thermal treatment at 100°C in an oven. This means that by the annealing process, just the cold crystallisation of the PLA material could be influenced.

Crystallinity values of all PLA and PLA/wood specimens were calculated from the first DSC heating scan that correlated with the thermal history coming from the process, 3D printing or injection moulding. The values of calculated crystallinities are shown in Figure 7.

As shown in Figure 7, the values of crystallinity were always slightly higher after water storage experiments for all PLA and PLA/wood composites processed by both methods. The reason for that could be the increased mobility of PLA polymer chains caused by presence of water. In Figure 8, an example is shown for how the total crystallinity value of PLA and PLA/wood composites was calculated.

Besides the crystallinity, specific thermal properties such as glass transition temperature ($T_g$), cold crystallisation temperature ($T_c$) and melting temperature ($T_m$) were also characterised via DSC. The results of the thermal characterisation could be found in Table II.

**Figure 7** Crystallinity values of PLA and PLA/Wood composites of 3D printed and injection moulded specimens before and after water storage

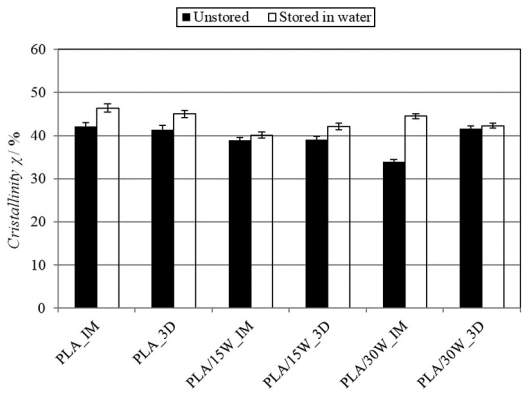


No significant differences in thermal properties, such as $T_g$, $T_c$ or $T_m$, between injection-moulded and 3D-printed samples could be determined. The amount of wood content did not influence these thermal properties either. Furthermore, the water storage test also did not influence $T_g$, $T_c$ or $T_m$.

## 4. Conclusions

In this study, the influence of water absorption on tensile properties and impact strength, as well as the morphology of PLA and PLA/wood composites prepared by injection moulding and 3D printing, was described. Owing to the nature of these processes, injection-moulded and 3D-printed samples showed significant differences in mechanical properties after being stored in water for seven days. The tensile strength and stiffness were significantly reduced by the softening effect of water inside the tested PLA and PLA/wood samples. The influence of the water storage increased with higher content of wood in the PLA composites. This was true for all measured mechanical properties.

**Table II** Thermal properties of PLA and PLA/wood composites

| Code | $T_g$ [°C] | $T_c$ [°C] | $T_m$ [°C] |
|---|---|---|---|
| PLA_IM | 56.2 | 94.2 | 169.1 |
| PLA_3D | 56.5 | 94.1 | 168.3 |
| PLA/15W_IM | 55.8 | 94.6 | 168.5 |
| PLA/15W_3D | 55.9 | 94.4 | 168.8 |
| PLA/30W_IM | 56.1 | 94.3 | 168.7 |
| PLA/30W_3D | 56.1 | 94.5 | 168.4 |

The basic differences between injection-moulding and 3D-printing processes, such as high pressures and deformation rates during injection and very high and fast degree of cooling, led to a compact structure of the injection-moulded samples. This was not the case with 3D-printed samples that always showed the appearance of porous structures, as shown by CT measurements. One main reason was that 3D-printed samples were produced without external pressure when compared to injection-moulded samples. In general, the porous structure resulted in inferior mechanical properties. Furthermore, water was taken up to a higher amount. From this study, it could be learned that the differences in mechanical performance between 3D-printed and injection-moulded specimens were larger in the case of PLA/wood composites than with unfilled PLA. 3D-printed samples showed significantly lower mechanical properties than injection-moulded parts. This had to be taken into account when injection-moulded samples had to be replaced by 3D-printed samples because of the cost and time. For both injection-moulded and 3D-printed samples, the most measured mechanical properties were significantly reduced after seven days of storing in water; therefore, it could limit their application range as well. The higher the wood content in the produced parts, the higher was the reduction of mechanical properties in spite of the tensile modulus. This was not the case for unfilled PLA produced by both methods. Therefore, reduction of the mechanical performance of PLA/wood composites could be definitely attributed to the used wood flour.

**Figure 8** DSC 1st heating scan from injection moulded stored (PLA_IM_S) and unstored (PLA_IM_U) as well as unfilled PLA: Calculation of the melting enthalpies

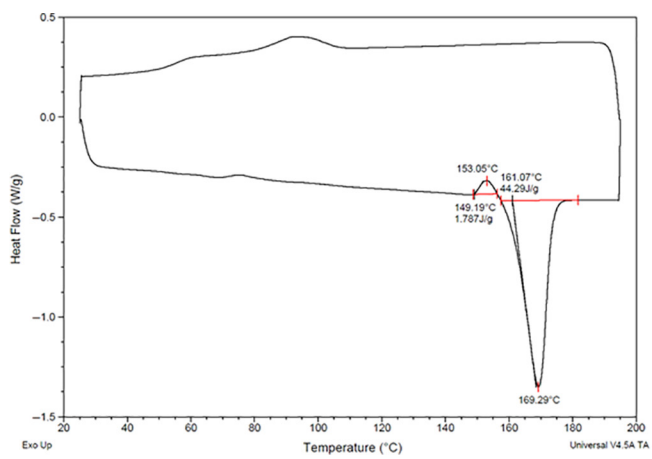


(a)

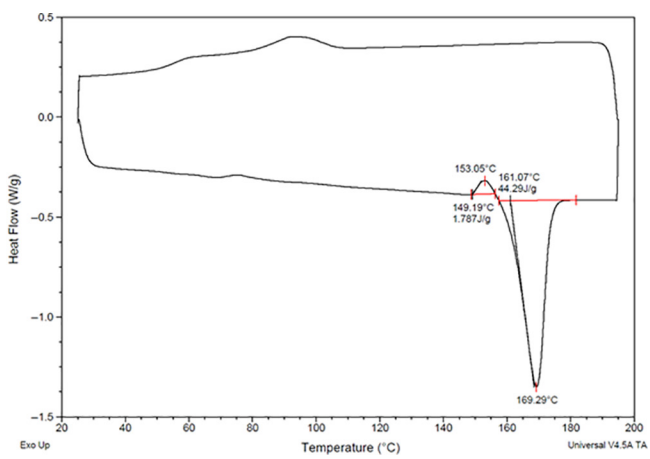


(b)

## References

Alvarez, V., Fraga, A. and Vázquez, A. (2004), "Effects of the moisture and fiber content on the mechanical properties of biodegradable polymer sisal fiber biocomposites", *Journal of Applied Polymer Science*, Vol. 91 No. 6, pp. 4007-4016.

Ecker, J.V., Fürst, C., Unterweger, C., Plank, B. and Haider, A. (2017), "3D computed tomography as quality control tool in advanced composite manufacturing", *Journal of Non-Destructive Testing*, id = 21944, available at: www.ndt.net/article/ctc2018/papers/ICT2018_paper_id156.pdf

Hoogsteen, W., Postema, A.R., Pennings, A.J. and Brinke, G. (1990), "Crystal structure, conformation and morphology of solution-spun poly (L-lactide) fibers", *Macromolecules*, Vol. 23 No. 2, p. 634.

Huda, M.S., Drzal, L.T., Misra, M. and Mohanty, A.K. (2006), "Wood-fiber-reinforced poly (lactic acid) composites: evaluation of the physico-mechanical and morphological properties", *Journal of Applied Polymer Science*, Vol. 102 No. 5, pp. 4856-4869.

Lorenza, A.T., Arnal, M.L., Albuerne, J. and Muller, A.J. (2007), "DSC isothermal polymer crystallization kinetics measurements and the use of the Avrami equation to fit the data: guidelines to avoid common problems", *Journal of Polymer Testing*, Vol. 26 No. 2, pp. 222-231.

Ndazi, B.S. and Karlsson, S. (2011), "Characterization of hydrolytic degradation of polylactic acid/rice hulls composites in water at different temperatures", *eXPRESS Polymer Letters*, Vol. 5 No. 2, pp. 119-131.

Retegi, A., Arbelaiz, A., Alvarez, P., Llano-Ponte, R., Labidi, J. and Mondragon, I. (2006), "Effects of hydrothermal ageing on mechanical properties of flax pulps and their polypropylene matrix composites", *Journal of Applied Polymer Science*, Vol. 102 No. 4, pp. 3438-3445.

Seguela, R. (2005), "Critical review of the molecular topology of semicrystalline polymers: the origin and assessment of intercrystalline tie molecules and chain entanglements", *Journal of Polymer Science Part B: Polymer Physics*, Vol. 43 No. 14, pp. 1729-1748.

Taib, R.M., Ramarad, S., Mohd Ishak, Z.A. and Todo, M. (2009), "Properties of kenaf fiber/polylactic acid biocomposites plasticized with polyethylene glycol", *Polymer Composites*, Vol. 31, pp. 1213-1222.

Vroman, I. and Tighzert, L. (2009), "Review: biodegradable polymers", *Materials*, Vol. 2 No. 2, pp. 307-344.

Yang, G., Su, J., Su, R. and Zhang, Q. (2012), "Toughening of PLA by annealing: the effect of crystal morphologies and modifications", *Journal of Macromolecular Science, Part B, Physics*, Vol. 51 No. 1, pp. 184-196.

Yew, G.H., Mohd Yusof, A.M., Mohd Ishak, Z.A. and Ishiaku, U.S. (2005), "Water absorption and enzymatic degradation of poly(lactic acid)/rice starch composites", *Polymer Degradation and Stability*, Vol. 90 No. 3, pp. 488-500.

## Corresponding author

**Josef Valentin Ecker** can be contacted at: Sirjiv@gmail.com